RSC Advances

PAPER

View Article Online
View Journal | View Issue

Cite this: *RSC Adv.*, 2017, **7**, 52304

Vapor phase aldol condensation of methyl acetate with formaldehyde over a Ba–La/Al_2O_3 catalyst: the stabilizing role of La and effect of acid–base properties†

Qiang Bao,[a] Wanchun Zhu,[a] Jianbiao Yan,[ab] Chunlei Zhang,[b] Chunli Ning,[b] Yi Zhang,[b] Mengmeng Hao[a] and Zhenlu Wang *[a]

Received 8th September 2017
Accepted 28th October 2017

DOI: 10.1039/c7ra10008f

rsc.li/rsc-advances

Vapor phase aldol condensation of methyl acetate with formaldehyde was studied over Ba–La/Al_2O_3 with different amounts of lanthanum catalysts. The catalysts were characterized by X-ray diffraction (XRD), N_2 adsorption–desorption, pyridine absorption performed *via* Fourier transform infrared spectroscope (Py-IR), NH_3 and CO_2 temperature-programmed desorption (NH_3 and CO_2-TPD), thermal analysis (TG-DTA) and scanning electron microscopy (SEM). The catalytic performance was evaluated using a fixed-bed microreactor. The results showed that bare Al_2O_3 was intrinsically active but poorly selective to methyl acrylate. The addition of barium species significantly improved the catalytic activity and selectivity. However, the Ba/Al_2O_3 catalyst was not stable in the continuous reaction due to a large amount of carbon deposition on the catalyst surface. Compared with adding individual components (BaO), the combination of the two promoters (BaO and La_2O_3) showed higher catalytic stability. Although the activity of the Ba–La/Al_2O_3 catalyst was not obviously increased compared with the Ba/Al_2O_3 catalyst, the carbon deposition was obviously suppressed in the target reaction due to the alkaline function of La_2O_3. Combined with the characterization results, we found that the addition of lanthanum species could significantly reduce the number of strong acid sites on the catalyst surface, inhibit the generation of carbon species in the reaction process, and stabilize the catalytic activity of the catalyst. In addition, the lifetime of the optimum 5Ba–0.5La/Al_2O_3 catalyst was evaluated over a continuous period of 300 h, and the initial catalytical activity did not exhibit an obvious decrease.

1. Introduction

As a fundamental industrial monomer, methyl acrylate (MA) is widely used in the manufacture of paint additives, adhesives, textiles, and leather treating agents.[1–4] The traditional way of producing MA is the acetone cyanohydrin (ACH) process.[5,6] This route requires large quantities of toxic hydrogen cyanide and produces copious amounts of ammonium sulfate wastes, which is unsustainable and environmentally unfriendly. Commercially, MA is produced by esterification of acrylic acid (AA) and methanol, prior to the synthesis of AA by the two-stage oxidations of propylene with air.[7–11] However, propylene comes from non-sustainable sources in the petrochemical industry, and the price of it is greatly influenced by the crude oil price. With the ever increasing demand for petroleum, it is becoming increasingly to use propylene as a feedstock. Therefore, development of alternative routes for MA production is necessary. In recent decades, a one-step synthesis of AA and ester *via* a vapor-phase aldol condensation of acetic acid (Aa) or methyl acetate (Ma) with formaldehyde (FA) has been studied and developed.

According to previous work, there are two types of catalysts tested for the aldol condensation reaction: acidic catalysts and basic catalysts. Acidic catalysts consist mainly of oxides of metals such as vanadium(v) oxide (V_2O_5), phosphorus(v) oxide (P_2O_5), and niobium(v) oxide (Nb_2O_5). Early on, Ai[12–14] reported that both the vanadium–titanium binary phosphates and V_2O_5–P_2O_5 binary oxide can effectively catalyze the aldol condensation of HCHO with acetic acid/methyl acetate to acrylic acid and its derivative. Based on their work, Feng *et al.*[15] successfully prepared an improved VPO catalyst using benzyl alcohol and PEG additive, activated in a butane-containing atmosphere, and the optimal conversion of methyl acetate reached 84.2% (including 30–35% acetic acid and 3–12% CO_x). More attention has been paid to basic catalysts, which often include the oxides or hydroxides of alkali or alkaline earth metals supported on

[a]*Key Laboratory of Surface and Interface Chemistry of Jilin Province, College of Chemistry, Jilin University, Qianjin Road 2699, Changchun, 130012, PR China. E-mail: wzl@jlu.edu.cn; Fax: +86 431 88499140; Tel: +86 431 88499140*

[b]*Shanghai Huayi (Group) Company Technology Research Institute, Longwu Road 4600, Shanghai 200241, PR China*

† Electronic supplementary information (ESI) available. See DOI: 10.1039/c7ra10008f

porous materials, for vapor phase aldol condensation because of the easier preparation and higher catalytic activity than acidic catalysts. Yan *et al.*[16] used an SBA-15 mesoporous molecular support impregnated with cesium oxide (Cs_2O) to catalyze the aldol condensation of methyl acetate with formaldehyde, and the best catalyst demonstrated the highest (48.4%) conversion of methyl acetate with 95.0% selectivity for methyl acrylate. Zhu *et al.*[17] reported a Cs–La–Sb/SiO_2 catalyst and showed the conversion of methyl acetate (20%) as well as a yield of methyl acrylate (8%). Furthermore, they found that the activity of the best catalyst sharply decreased as the reaction progressed due to the loss of the Cs species. Recently, an Al_2O_3-supported cesium catalyst was reported to be a good base catalyst for the vapor phase aldol condensation of methyl acetate with formaldehyde. Zhang *et al.*[18] prepared a series of Cs–P/γ-Al_2O_3 catalysts, and the best catalyst demonstrated a 47.1% yield of methyl acrylate. However, the activity decreased quickly because of the carbon deposition on the surface of the catalyst. Then, they used the same catalyst system in a fluidized bed reactor, and they found it had high catalytic stability, with no significant decrease in catalytic activity after 1000 h of lifetime evaluation.[19] However, it is well known that the catalytic reaction with fluidized bed has a series of problems such as severe catalyst loss, wear of reaction vessels and higher gas–solid separation requirements.

Previous studies have shown that the performance of alumina, although very good, is limited by the carbon deposition attached to the catalyst surface. The activity of the catalyst decreased quickly with the increase in carbon deposition. This phenomenon might be due, at least in part, to the strong surface acidity of alumina. As reported, the acidity of γ-Al_2O_3 was related to the degree of coordination of the Al^{3+} species, of which the strongest Lewis acid sites were associated with very lowest coordination Al cations, such as tri- and tetra coordinated Al^{3+}.[20–25] In addition, both strong solid acid and base sites were also ineffective in catalyzing the aldol condensation reaction, and the moderate acidity corresponded to higher selectivity.[26] Thus, it is necessary to reduce the surface acidity of γ-Al_2O_3 not only in inhibiting the formation of coke but also in improving the catalytic activity. Doping of alumina with basic components could be an efficient way to improve the catalytic stability and resistance to coking.[27–29]

In this paper, vapor-phase aldol condensation of methyl acetate with formaldehyde was studied over a series of Ba–La/Al_2O_3 catalysts. Metal-modified catalysts were prepared for inhibiting carbon accumulation and stabilizing the catalytic activity. The physical–chemical properties of the catalysts were studied by N_2-adsorption and X-ray diffraction (XRD). The surface acidity and basicity of the catalysts were studied by CO_2-TPD, NH_3-TPD and pyridine adsorption IR. Catalytic tests were carried out in a fixed-bed microreactor. Additionally, the effect of the lanthanum loading amounts of the aldol condensation of Ma and FA were investigated under the same conditions. The carbon deposition of the used catalysts with or without lanthanum promotion was studied by thermal analysis (TG-DTA) and scanning electron microscopy (SEM). The stability and regeneration of the optimum catalyst were also investigated.

2. Experiment

2.1 Catalyst preparation

Methyl acetate (≥99.0%), methanol (CH_3OH; ≥99.0%), trioxymethylene (≥98.0%), barium acetate ($Ba(CH_3COO)_2$; ≥99.0%), lanthanum nitrate hexahydrate (corresponding La_2O_3 content ≥44.0%) and alumina nitrate nonahydrate ($Al(NO_3)_3\cdot 9H_2O$ ≥ 99.0%) of analytical grade were purchased from the Sinopharm Chemical Reagent Company. The Al_2O_3 were prepared by precipitation of $Al(NO_3)_3\cdot 9H_2O$ from an aqueous solution with NH_3. The precipitates were thoroughly washed with deionized water at least three times, dried in an oven at 100 °C overnight and calcined in a muffle furnace at 500 °C for 5 h with a 2 °C min^{-1} heating ramp rate.

The Ba/Al_2O_3 catalysts were prepared with the wetness impregnation method. Typically, Al_2O_3 was impregnated with an aqueous solution with a desired amount of barium acetate, and the mixture was later stirred for approximately 2 h at room temperature. Afterwards, water in the mixture was evaporated at a temperature of 80 °C under atmospheric pressure. The dried materials were next calcined in a muffle furnace at 550 °C for 5 h with a 10 °C min^{-1} heating ramp rate. Ba–La/Al_2O_3 catalysts were prepared in the same way except that two aqueous solutions of $Ba(CH_3COO)_2$ and $La(NO_3)_3\cdot 6H_2O$ were mixed before impregnation. The catalysts were denoted as *x*Ba–*y*La/Al_2O_3, where *x* represents the content of Ba (wt%) and *y* represents the content of La (wt%). The 5Ba–0.5La/Al_2O_3 catalyst was prepared as follows: the Al_2O_3 supports (5 g) were impregnated with 4 ml of an aqueous solution containing the desired amount of $Ba(CH_3COO)_2$ (0.4407 g) and $La(NO_3)_3\cdot 6H_2O$ (0.0703 g). The other catalysts were prepared in the same way.

2.2 Catalyst characterization

X-ray diffraction patterns were measured with an Empyrean X-ray diffractometer using a nickel filtered Cu Kα source at a wavelength of 0.154 nm. An accelerating voltage of 40 kV and a current of 40 mA were used. A slit width of 0.25° was used as the source. Scans were collected using a PIXcel3D detector. N_2 adsorption/desorption isotherms were measured using a Micromeritics ASAP 2010N analyzer. Specific surface areas were calculated using the BET model. Pore size distributions were evaluated from desorption branches of nitrogen isotherms using the BJH model. The carbon deposition on spent catalysts was examined by thermal analysis, using a Germany NETZSCH thermoanalyzer (model STA 499F3). The spent samples (10 mg) were heated at a rate of 10 °C min^{-1} from room temperature to 900 °C in an air flow of 10 cm^3 min^{-1}. Scanning electron microscopy observations of the fresh and the spent catalyst samples were performed using a Hitachi SU8020. Temperature programmed desorption of NH_3 and CO_2 was used to characterize the acidic and basic sites over the studied catalysts, respectively. The TPD experiments were conducted using a ChemBET Pulsar TPR/TPD instrument (Quantachrome Instruments) with a built-in TCD detector. Typically, a 50 mg catalyst was used in each measurement. The catalyst was first purged with He (UHP grade, Airgas) at 550 °C for 0.5 h with

a 10 °C min^{-1} heating ramp rate, then cooled down to 50 °C. A flow of CO_2 (research grade, Airgas) or NH_3 (electronic grade, Airgas) was introduced into the tubular catalyst bed for 30 min at 50 °C for CO_2 adsorption and 50 °C for ammonia adsorption. After purging the catalyst bed for approximately 30 min with He to evacuate the physisorbed NH_3 or CO_2, the catalyst was heated to 550 °C with a 10 °C min^{-1} heating ramp rate. The change in thermal conductivity due to the concentration change of NH_3 or CO_2 in the effluent was recorded on the TCD detector. The TPD profile was deconvoluted using a Gaussian multipeak fitting function built-in OriginPro7.5 software. IR spectra were recorded on a Nicolet Impact spectrometer at 4 cm^{-1} optical resolution. Prior to the measurements, 30 mg of the catalyst was pressed in self-supporting discs and activated in the IR cell attached to a vacuum line at 250 °C for 0.5 h. The adsorption of pyridine (Py) was performed at 50 °C for 30 min. The excess of pyridine was further evacuated at 50 °C for 0.5 h. After elimination of the physical absorption the sample was cooled to room temperature for registration of the IR spectra, and the sample was returned to reaction conditions and heated to a further temperature.

2.3 Catalyst evaluation

The vapor phase aldol condensation reaction of methyl acetate with formaldehyde was conducted in a fixed-bed reactor under atmospheric pressure. The reason why we choose a fixed bed reactor is that it has a small amount of catalyst and a small reaction volume to achieve greater production capacity. And it can strictly control the time of stay, reaction temperature and other parameters, which are more conducive to the study of the performance of the catalyst. Typically, 500 mg of catalyst was loaded at the center of a stainless steel tube reactor that was 30 cm long with a 0.8 cm inside diameter and supported by a quartz frit. The mixed solution of methyl acetate and formaldehyde was fed into the reactor using an advection pump with a typical flow rate of 0.06 mL min^{-1}. The products were identified and analyzed by gas chromatography (GC-8A, FID) equipped with a 60 m capillary column DB-WAX. Some GC data for the catalytic reaction have been added to ESI (in Fig. S1†).

The molar ratio of Ma and FA was fixed at 1/2 unless otherwise indicated. The catalysts were evaluated based on their catalytic performance. The definition of methyl acetate conversion and product selectivity was as follows:

$$\text{Ma conversion (\%)} = (\text{Ma}_{in} - \text{Ma}_{out})/\text{Ma}_{in} \times 100$$

$$\text{MA selectivity (\%)} = \text{MA}/(\text{Ma}_{in} - \text{Ma}_{out}) \times 100$$

$$\text{MA yield (\%)} = \text{Ma conversion (\%)} \times \text{MA selectivity (\%)}$$

3. Results and discussion

3.1 Physical properties

The surface area and pore size distribution of Ba–La/Al_2O_3 catalysts were analyzed using N_2 adsorption–desorption. Fig. 1 shows that both Al_2O_3 and metal-modified Al_2O_3 were type IV with an H1-type hysteresis loop at high relative pressure. All of the textural properties of Ba–La/Al_2O_3 samples are depicted in Table 1. From Table 1, we can see the specific surface area of Al_2O_3 decreased obviously with the addition of 5 wt% BaO. Although the pore volume changed minimally, the pore diameter increased significantly, indicating that Ba species produced changes in the textural properties of the alumina support. For Ba–La-modified catalysts, the specific surface area of Ba–La/Al_2O_3 progressively decreased with increasing lanthanum content. The pore volume of the catalysts did not change significantly, whereas the pore diameter increased gradually. This finding suggests that during the impregnation procedure, there was some dissolution and precipitation of oxides with blockage of smaller pores. However, it should be noted that the specific surface area of Ba–La-modified Al_2O_3 catalysts was obviously higher than that of the 5Ba/Al_2O_3 catalyst, indicating that the addition of small quantities of lanthanum species may help to limit the decrease in the S_{BET} of Ba/Al_2O_3.

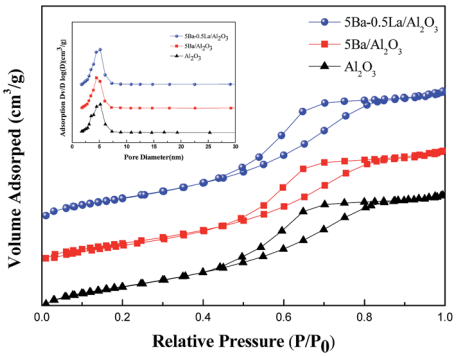

Fig. 1 N_2 adsorption–desorption isotherms and pore-size distribution of studied catalysts.

The XRD patterns of the samples are presented in Fig. 2. From Fig. 2, we can see that the diffraction peaks of the Al_2O_3 support were broad and diffuse, which means the amorphous alumina is the main existing form. For the 5Ba/Al_2O_3 sample, no diffraction peaks due to Ba species are detected, which is consistent with prior studies.[30] As the content of lanthanum increased from 0 to 3.0 wt%, the XRD patterns of Ba–La/Al_2O_3 showed only the reflections of the Al_2O_3 support material. This finding means that lanthanum species are highly dispersed on the surface of Al_2O_3.

Table 1 Textural properties of the Al_2O_3 and metal-modified Al_2O_3 catalysts

Catalysts	S_{BET} (m^2 g^{-1})	Pore volume (cm^3 g^{-1})	Mean pore diameter (nm)
Al_2O_3	307.7	0.42	5.4
5Ba/Al_2O_3	272.3	0.41	6.0
5Ba–0.1La/Al_2O_3	299.4	0.44	5.8
5Ba–0.5La/Al_2O_3	292.6	0.44	6.0
5Ba–1.0La/Al_2O_3	290.6	0.43	5.9
5Ba–3.0La/Al_2O_3	286.4	0.45	6.2

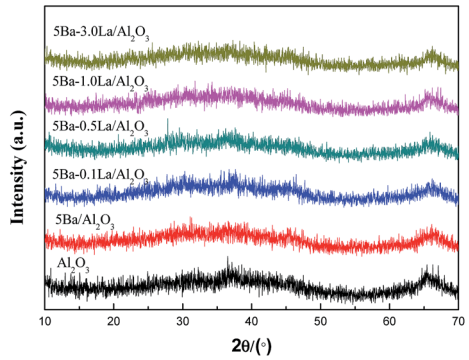

Fig. 2 The XRD patterns of Al_2O_3 and metal-modified Al_2O_3 catalysts.

3.2 Acid–base properties

The acid–base properties of the Al_2O_3 and metal-modified Al_2O_3 were characterized by the TPD of NH_3–CO_2 in Fig. 3 and Fig. 4. Table 2 lists the total CO_2 and NH_3 uptakes on the basis of catalyst weight and the corresponding concentrations for the different types of acid/base sites. In Fig. 3, all NH_3-TPD profiles were integrated (deconvoluted) in six fixed temperature ranges (100–215 °C, 215–250 °C, 250–290 °C, 290–330 °C, 330–365 °C and 365 °C ~) in order to compare acidic sites of the same strength. For support, a very large amount of NH_3 uptake

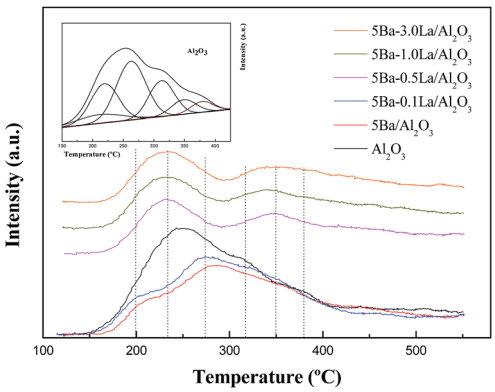

Fig. 3 NH_3-TPD patterns of the studied catalysts.

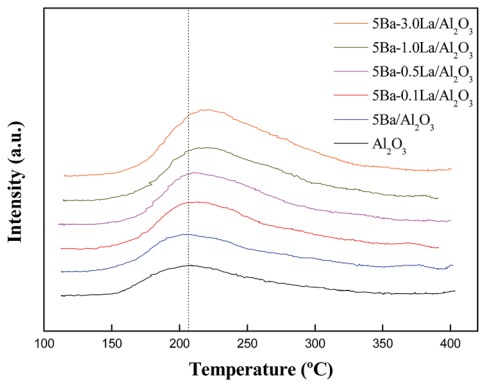

Fig. 4 CO_2-TPD patterns of the studied catalysts.

(103.6 μmol g^{-1} cat.) was observed over Al_2O_3, probably due to the rich Lewis acid sites from coordinative unsaturated aluminum ions on the catalyst surface. The alumina supported BaO catalyst had a dramatically decreased NH_3 uptake at a temperature of 100–330 °C (90.3 μmol g^{-1} cat. for bare Al_2O_3 and 48.4 μmol g^{-1} cat. for $5Ba/Al_2O_3$), indicating that a large number of weak acid sites were reduced when BaO was supported on Al_2O_3. According to previous reports, for γ-Al_2O_3, bulk Al atoms display either tetrahedral or octahedral coordination. Exposed surface Al sites can display three-, four-, or 5-fold coordination, and exhibit Lewis acidity, of which the weakest Lewis acid sites were associated with very high coordination Al cations, such as 5-coordinated Al^{3+}.[25,29] Thus, the reduction of weak acid sites may be due to the interaction between BaO and 5-coordinated Al^{3+}. J. Kwak and co-workers found the BaO could selectively anchor the penta-coordinated Al^{3+} sites on the (100) facets of γ-Al_2O_3.[31] This finding was consistent with our experimental results. For Ba–La/Al_2O_3 catalysts, the total NH_3 uptake over $5Ba–0.1La/Al_2O_3$ was approximately 75.4 μmol g^{-1} cat., slightly more than the NH_3 uptakes for $5Ba/Al_2O_3$ (61.4 μmol g^{-1} cat.), indicating that adding a small amount of lanthanum could increase total acid content. More interestingly, the NH_3 uptake over $5Ba–0.5La/Al_2O_3$ at a temperature of 215–250 °C increased about 7.6 μmol g^{-1} catalyst compared to $5Ba/Al_2O_3$. However, the NH_3 uptake in other temperature ranges (especially at a temperature of 330–365 °C) decreased dramatically. It might be the result of an interaction between lanthanum species and acid sites on the catalyst surface, leading to an increase in weak acid sites and a decrease in strong acid sites. With a further increase of lanthanum species, the NH_3 uptake at all the temperature ranges did not changed significantly. Fig. 4 shows the desorption profiles of CO_2 from Ba–La/Al_2O_3 catalysts with different amounts of lanthanum. From Fig. 4, we can see that all catalysts exhibited a prominent CO_2 desorption peak in the range of 100–350 °C and the basic sites on these catalysts were arbitrarily considered weak. Adding barium species slightly increased the total CO_2 uptake (10.1 μmol g^{-1} cat.) compared to the Al_2O_3 support (8.3 μmol g^{-1} cat.). It should be noted that adding lanthanum could also increase the total CO_2 uptake from 13.3 μmol g^{-1} cat. for $5Ba–0.1La/Al_2O_3$ to 18.4 μmol g^{-1} cat. for $5Ba–3.0La/Al_2O_3$. Furthermore, the CO_2 adsorption capacity of Ba–La/Al_2O_3 catalysts gradually increased with a further increase in lanthanum species, indicating some new stronger base sites formed on the catalyst surface.

To determine the nature of the acidic sites, the acid properties of the Al_2O_3 and metal-modified Al_2O_3 were further characterized by FTIR spectra of pyridine adsorption. In Fig. 5, several feature bands were observed at 1446, 1490 and 1614 cm^{-1} on these samples, and their intensities became weaker when adding metal to the Al_2O_3 supports. The bands at 1446 and 1614 cm^{-1} could be attributed to pyridine adsorbed on Lewis acid sites. The band at 1490 cm^{-1} was also attributed to Lewis acid sites because there was no evidence for the formation of pyridinium ions at 1540 cm^{-1}. The IR results indicated that the surface of the Al_2O_3 and metal-modified Al_2O_3 catalysts mainly consist of Lewis acid sites. Furthermore, the relative amount of these sites declined when adding metal to the Al_2O_3 supports.

Table 2 List of the total CO_2 and NH_3 uptakes on the catalysts surface and the corresponding concentrations for the different types of acid/base sites

Catalyst	Al_2O_3	$5Ba/Al_2O_3$	$5Ba–0.1La/Al_2O_3$	$5Ba–0.5La/Al_2O_3$	$5Ba–1.0La/Al_2O_3$	$5Ba–3.0La/Al_2O_3$
Total (μmol NH_3 per g cat.)	103.6	61.4	75.4	38.5	39.9	40.2
T_1 (100–215 °C)	8.1	4.6	6.5	3.8	3.8	3.8
T_2 (215–250 °C)	25.5	8.1	11.2	15.7	16.0	15.7
T_3 (250–290 °C)	36.9	24.1	30.0	6.6	6.8	6.9
T_4 (290–330 °C)	19.8	11.6	13.7	4.2	4.7	4.8
T_5 (330–365 °C)	8.7	8.8	10.1	5.9	6.0	5.9
T_6 (>365 °C)	4.6	4.2	3.9	2.3	2.6	3.1
Total (μmol CO_2 per g cat.)	8.3	10.1	13.3	14.4	15.0	18.4
T_1 (100–350 °C)	8.3	10.1	13.3	14.4	15.0	18.4

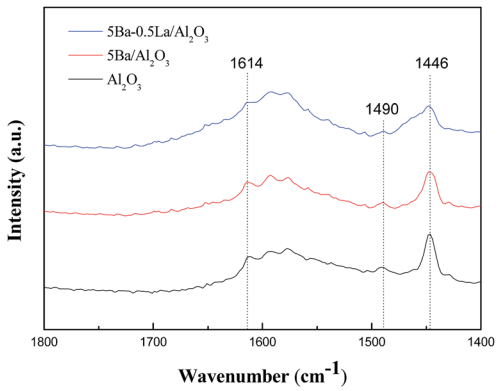

Fig. 5 FTIR spectra of pyridine adsorbed on Al_2O_3, $5Ba/Al_2O_3$ and $5Ba–0.5La/Al_2O_3$.

3.3 The characterization of used catalysts

The TG-DTA analysis of the catalyst samples used for 10 h in the aldol condensation of methyl acetate with formaldehyde at 390 °C and atmospheric pressure is presented in Fig. 6. TG analysis showed that weight losses were approximately 47%, 28% and 24% for the Al_2O_3, $5Ba/Al_2O_3$ and $5Ba–0.5La/Al_2O_3$ catalysts, respectively, indicating a significant amount of carbon deposition on the Al_2O_3. The addition of BaO to Al_2O_3 obviously improved the carbon formation on the Al_2O_3 catalyst, which might be due to the reduction of acid sites. The smallest amount of carbon deposition was found on the $5Ba–0.5La/Al_2O_3$ catalyst after the reaction for 10 h, indicating that adding a small amount of lanthanum could further prevent carbon deposition for aldol condensation of methyl acetate with formaldehyde. In the DTA curves, there were two exothermic peaks at 400 and 480 °C for Al_2O_3 samples, two exothermic peaks at 395 and 460 °C for $5Ba/Al_2O_3$ samples, and one broader exothermic peak at 385–450 °C for $5Ba–0.5La/Al_2O_3$ samples. These findings indicate that two different carbon deposition species on these catalysts were oxidized and that the carbon deposition species on the Al_2O_3 with BaO and La_2O_3 promoters were more easily oxidized than that on the Al_2O_3 catalyst. Thus, the temperature of the exothermic peaks for carbon deposition oxidation on the Al_2O_3 with BaO and La_2O_3 promoters was lower than that on the Al_2O_3 catalyst.

Coke formation was also confirmed by SEM images as shown in Fig. 7. Fig. 7 shows SEM images of the Al_2O_3 catalyst (Fig. 7a and b), the $5Ba/Al_2O_3$ catalyst (Fig. 7c and d), and the $5Ba–0.5La/Al_2O_3$ catalyst (Fig. 7e and f) before and after the condensation reaction for 10 h at 390 °C and atmospheric pressure. From

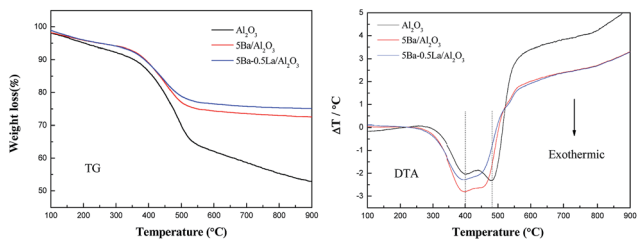

Fig. 6 TG and DTA curves of Al_2O_3, $5Ba/Al_2O_3$ and $5Ba–0.5La/Al_2O_3$.

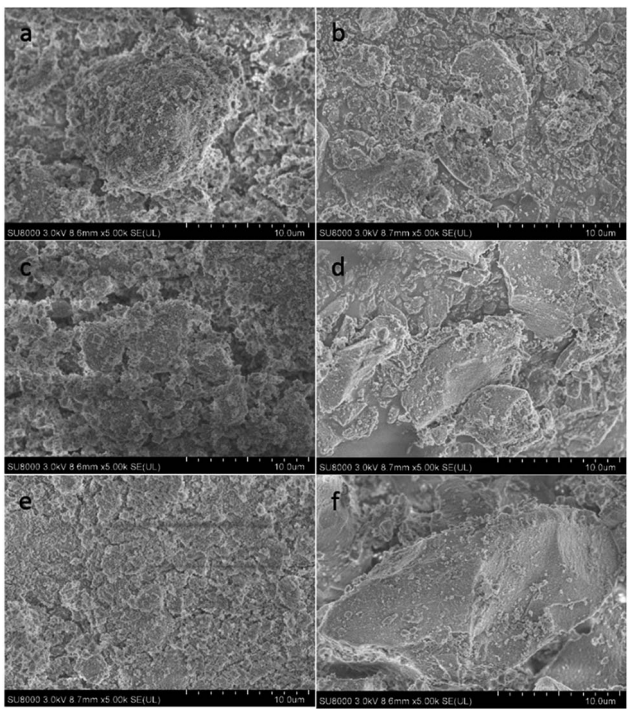

Fig. 7 SEM micrographs of the catalysts before and after reaction for 10 h at 390 °C (a and b) before and after reaction on Al_2O_3; (c and d) before and after reaction on $5Ba/Al_2O_3$; (e and f) before and after reaction on $5Ba–0.5La/Al_2O_3$.

Fig. 7, it can be seen that the surface of the fresh catalyst is porous and rough. The hole is clearly visible. However, the surface of the spent catalyst is relatively smooth, and the channel is seriously blocked. Furthermore, there are some particles of new, uniform material produced on the surface of the spent catalyst. The reason for these results is that the catalyst is covered with a large amount of carbon deposition during the reaction, thereby blocking the pore structure of the catalyst surface.

3.4 Activity tests

Different dopants including rare earth metals, alkali metals and other elements were also prepared *via* the same impregnation method. The evaluation result is shown in Table S1.† It can be observed that the 5Ba–0.5La/Al_2O_3 catalyst showed the best catalytic performance. Garbarino *et al.*[32] studied the ethanol conversion reaction on the La–alumina catalysts. They found that the addition of lanthanum could stabilize alumina with respect to sintering and loss of surface area, as well as against carbon laydown. Furthermore, they also suggested that the La^{3+}–O^{2-} couples interact specifically with the strongest acido–basic sites of alumina reducing the Lewis acidity but providing moderate acido–basic couples. And in our previous studies, we have shown that the medium acid–base sites is more suitable for the aldol condensation reaction.[33] Therefore, we only reported the Ba–La-modified Al_2O_3 catalysts. The evaluation results of the studied catalysts are presented in Fig. 8. From Fig. 8, bare Al_2O_3 was found to be intrinsically active but poorly selective to methyl acrylate. With the addition of 5 wt% BaO to the Al_2O_3 support, the 5Ba/Al_2O_3 catalyst showed an obvious increase in catalytic activity to methyl acetate. Furthermore, the selectivity for methyl acrylate increased 13.4% compared to the bare Al_2O_3. This result is agreement with our previous research.[33] When adding 0.5 wt% La_2O_3 to 5Ba/Al_2O_3, the 5Ba–0.5La/Al_2O_3 catalyst did not show a marked increase in catalytic activity and selectivity. However, it should be noted that, compared with adding individual components, a combination of the two promoters showed higher catalytic stability since the decline in catalytic activity in 5Ba–0.5La/Al_2O_3 was not so sharp as in 5Ba/Al_2O_3 and Al_2O_3. From the NH_3-TPD analysis, the addition of lanthanum species significantly altered the acid environment of the catalyst surface. An appropriate amount of lanthanum species (5Ba–0.5La/Al_2O_3) can not only effectively reduce the amount of strong acid, but also produce more weak acid sites corresponding to NH_3 uptake at a temperature of 215–250 °C in our study. The TG-DTA analysis showed that the 5Ba–0.5La/Al_2O_3 catalyst had the least amount of carbon produced after 10 h compared with the Al_2O_3 and 5Ba/Al_2O_3 catalysts. It is well known that carbon deposition (or coking) is one of the principal factors that may deactivate catalysts.[34–36] Zhu *et al.*[17] studied the compositions of soluble coke on the Cs–La–Sb/SiO_2 catalyst. They found that the composition of soluble coke in deactivated catalysts was mainly aromatic hydrocarbon. Toluene, DMBs, TriMBs and hextraMB were all detected. Furthermore, they also found that the addition of lanthanum species was conducive to the inhibition of carbon formation due to covering strong acid sites and providing weak acid sites. This conclusion is exactly consistent with our present study. Therefore, combined with the catalytic activity and characterization results, we can conclude that the addition of lanthanum species reduced the number of strong acid sites on the catalyst surface, inhibited the generation of carbon species in the reaction process, and stabilized the catalytic activity of the catalyst.

To investigate the effect of the lanthanum loading amounts on the aldol condensation reaction of methyl acetate with formaldehyde, the Ba–La/Al_2O_3 catalysts with different lanthanum content were also prepared by the same preparation method. The evaluation results of the studied catalysts are shown in Fig. 9. From Fig. 9, we can see that with the increase in lanthanum content, the activity and selectivity of the catalysts did not change much, but the stability of the Ba–La/Al_2O_3 catalysts had been obviously improved. When adding 0.5 wt% La_2O_3 to 5Ba/Al_2O_3, the stability of the obtained catalyst was the best. The specific stability order of studied catalysts was as follows: 5Ba–0.5La/Al_2O_3 > 5Ba–1.0La/Al_2O_3 > 5Ba–0.1La/Al_2O_3 ≈ 5Ba–3.0La/Al_2O_3. From the CO_2-TPD analysis, with the addition of lanthanum species, the number of basic sites on the catalyst surface gradually increased, and the center of the desorption peak was shifted toward the high-temperature zone, which indicated that some new stronger basic sites were generated on the catalyst surface. In our previous studies, the proper acid–base properties, such as the number and strength of the catalysts, were critical to promoting this aldol condensation reaction.[33] Therefore, too much or too little load may cause the acid–base environment of the catalyst to not be suitable for the target reaction.

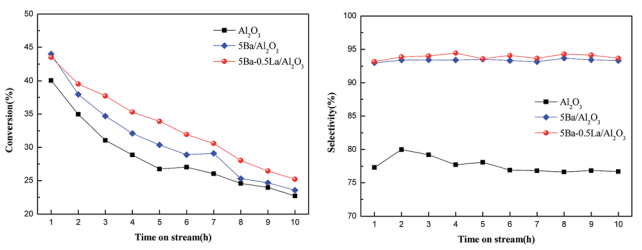

Fig. 8 The conversation of Ma and the selectivity to MA on the Al_2O_3, 5Ba/Al_2O_3, and 5Ba–0.5La/Al_2O_3 catalysts.

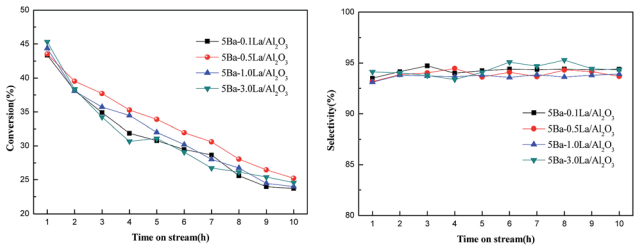

Fig. 9 The conversation of Ma and the selectivity to MA on the Ba–La/Al_2O_3 catalysts with different La content.

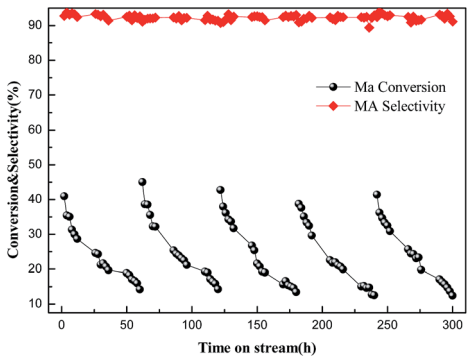

Fig. 10 The conversation of Ma and the selectivity to MA on the 5Ba–0.5La/Al_2O_3 catalyst. Note: the volume of feedstock is 0.03 ml min^{-1}.

3.5 Catalyst stability and reusability

The stability and regeneration of the 5Ba–0.5La/Al_2O_3 catalyst were also investigated at 390 °C for about 300 h, and the results are shown in Fig. 10. The catalyst was regenerated by calcining in a stream of air at 550 °C for 5 h and studied under the same conditions. From Fig. 10, we can see that Ma conversion declined by nearly 60% after reaction at 60 h. In fact, the catalyst turned brown and black after the reaction. According to the results of TG-DTA and SEM analysis, we can conclude that the deactivation of catalyst can be due to the formation of carbon deposition on the surface of the catalyst.[18,34,36]

Although the activity (based on the conversation of Ma) decreased gradually with reaction time as the result of the formation of carbonaceous deposits, the regenerated catalyst, by removing carbonaceous deposits at high temperatures in a stream of air, showed nearly the same initial catalytic activity as the fresh catalyst. This result indicated that the effective components of the regenerated catalyst were not destroyed in the process of regeneration, and the activity of the 5Ba–0.5La/Al_2O_3 catalyst was relatively stable after a total reaction time of 300 h. Thus, the 5Ba–0.5La/Al_2O_3 catalyst really had good reusability.

4. Conclusions

Vapor phase aldol condensation of methyl acetate and formaldehyde was investigated over Ba–La/Al_2O_3 catalysts in a fixed-bed reactor. The properties of the catalysts and the carbon deposition performance on the catalyst surface were surveyed by XRD, N_2 adsorption–desorption, TG-DTA, and SEM. The acid–base properties of the catalysts were characterized by TPD of NH_3–CO_2 and FTIR spectra of pyridine adsorption. The results of the catalyst evaluation showed that the 5Ba–0.5La/Al_2O_3 catalyst exhibited the best catalytic activity and selectivity on the aldol condensation of methyl acetate with formaldehyde, and the conversion of Ma achieved 39.5% and the selectivity of Ma achieved 93.9%. Although the activity of the 5Ba–0.5La/Al_2O_3 catalyst was not obviously increased compared with 5Ba/Al_2O_3 catalyst, the carbon deposition was greatly suppressed in the target reaction due to the alkaline function of La_2O_3. The IR results indicated that the surface of the Al_2O_3 and metal-modified Al_2O_3 catalysts mainly consisted of Lewis acidic sites. Furthermore, the relative amounts of these sites declined when adding metal to the Al_2O_3 supports. The results of the NH_3-TPD showed that the addition of lanthanum species can cause an increase in weak acid sites and a decrease in strong acid sites, making the surface acidity of the catalyst more suitable for the condensation reaction. The CO_2-TPD analysis showed that adding lanthanum species could also increase total CO_2 uptake, indicating that some new base sites formed on the catalyst surface. Furthermore, the quantitative results further demonstrated the changes in the acid–base environment on the catalyst surface. Combining the catalytic activity and selectivity with the characterization results, it can be concluded that the addition of lanthanum species significantly reduced the number of strong acid sites on the catalyst surface, inhibited the generation of carbon species in the reaction process, and stabilized the catalytic activity of the catalyst.

Conflicts of interest

There are no conflicts to declare.

Acknowledgements

This work was supported by the technology institute of Shanghai Huayi (Group) Company and Jilin Province Science and Technology research plan (key scientific research project). (No. 20150204020GX).

Notes and references

1 H. Danner, M. Dürms, M. Gartner and R. Braun, *Appl. Biochem. Biotechnol.*, 1998, **70**, 887.
2 X. Xu, J. Lin and P. Cen, *Chin. J. Chem. Eng.*, 2006, **14**, 419.
3 K. Nagai, *Appl. Catal., A*, 2001, **221**, 367.
4 P. Nagai and L. Lochmann, *Prog. Polym. Sci.*, 1999, **24**, 793–873.
5 E. Hauptman, S. Sabo-Etienne, P. White, M. White, J. Gamer, P. Fagan and J. Calabrese, *J. Am. Chem. Soc.*, 1994, **116**, 8038–8060.
6 M. Bacaa, M. Aouine, J. Dubois and J. Millet, *J. Catal.*, 2005, **233**, 234.
7 B. Jo, S. Kum and S. Moon, *Appl. Catal., A*, 2010, **378**, 76–82.
8 R. d'Alnoncourt, L. Csepei, M. Hävecker, F. Girgsdies, M. Schustera, R. Schlögl and A. Trunschke, *J. Catal.*, 2014, **311**, 369–385.
9 Z. Zhai, A. Getsoian and A. Bell, *J. Catal.*, 2013, **308**, 25–36.
10 W. Fang, Q. Ge, J. Yu and H. Xu, *Ind. Eng. Chem. Res.*, 2011, **50**, 1962–1967.
11 M. Hävecker, S. Wrabetz, J. Kröhnert, L. Csepei, R. d'Alnoncourt, Y. Kolen'ko, F. Girgsdies, R. Schlögl and A. Trunschke, *J. Catal.*, 2012, **285**, 48–60.
12 M. Ai, *J. Catal.*, 1987, **107**, 201–208.
13 M. Ai, *J. Catal.*, 1988, **112**, 194–200.
14 M. Ai, *Stud. Surf. Sci. Catal.*, 1992, **72**, 101–108.
15 X. Feng, B. Sun, Y. Yao, Q. Su, W. Ji and C.-T. Au, *J. Catal.*, 2014, **314**, 132–141.

16 J. Yan, C. Zhang, C. Ning, Y. Tang, Y. Zhang, L. Chen, S. Gao, Z. Wang and W. Zhang, *J. Ind. Eng. Chem.*, 2015, **25**, 344.
17 Y. Wang, X. Lang, G. Zhao, H. Chen, Y. Fan, L. Yu, X. Ma and Z. Zhu, *RSC Adv.*, 2015, **5**, 32826.
18 G. Zhang, H. Zhang, D. Yang, C. Li, Z. Peng and S. Zhang, *Catal. Sci. Technol.*, 2016, **6**, 6417.
19 S. Jiang, C. Li, H. Chen, D. Yang and S. Zhang, *Ind. Eng. Chem. Res.*, 2017, **56**, 9322–9330.
20 M. Digne, P. Sautet, P. Raybaud, P. Euzen and H. Toulhoat, *J. Catal.*, 2002, **211**, 1–5.
21 M. Digne, P. Sautet, P. Raybaud, P. Euzen and H. Toulhoat, *J. Catal.*, 2004, **226**, 54–68.
22 T. Phung, A. Lagazzo, M. Crespo, V. Escribano and G. Busca, *J. Catal.*, 2014, **311**, 102–113.
23 G. Jenness, M. Christiansen, S. Caratzoulas, D. Vlachos and R. Gorte, *J. Phys. Chem. C*, 2014, **118**, 12899–12907.
24 J. Hu, S. Xu, J. Kwak, M. Hu, C. Wan, Z. Zhao, J. Szanyi, X. Bao, X. Han, Y. Wang and C. Peden, *J. Catal.*, 2016, **336**, 85.
25 M. Christiansen, G. Mpourmpakisv and D. Vlachos, *ACS Catal.*, 2013, **3**, 1965–1975.
26 J. Tai and R. Davis, *Catal. Today*, 2007, **123**, 42–49.
27 B. Bloch, B. Ravi and R. Chaim, *Mater. Lett.*, 2000, **42**, 61–65.
28 J. Kwak, J. Hu, A. Lukaski, D. Kim, J. Szanyi and C. Peden, *J. Phys. Chem. C*, 2008, **112**, 9486–9492.
29 S. Bai, Q. Dai, X. Chu and X. Wang, *RSC Adv.*, 2016, **6**, 52564.
30 J. Kwak, D. Mei, C. Yi, D. Kim, C. Peden, L. Allard and J. Szanyi, *J. Catal.*, 2009, **261**, 17–22.
31 J. Kwak, J. Hu, D. Kim, J. Szanyi and C. Peden, *J. Catal.*, 2007, **251**, 189–194.
32 G. Garbarino, C. Wang, I. Valsamakis, S. Chitsazan, P. Riani, E. Finocchio, M. Flytzani-Stephanopoulos and G. Busca, *Appl. Catal., B*, 2017, **200**, 458–468.
33 Q. Bao, T. Bu, J. Yan, C. Zhang, C. Ning, Y. Zhang, M. Hao, W. Zhang and Z. Wang, *Catal. Lett.*, 2017, **147**, 1540–1550.
34 J. Cueto, L. Faba, E. Díaz and S. Ordónez, *Appl. Catal., B*, 2017, **201**, 221–231.
35 N. Miletić, U. Izquierdo, I. Obregón, K. Bizkarra, I. Agirrezabal-Telleria, L. Bario and P. Arias, *Catal. Sci. Technol.*, 2015, **5**, 1704–1715.
36 C. Sararuk, D. Yang, G. Zhang, C. Li and S. Zhang, *J. Ind. Eng. Chem.*, 2017, **46**, 342–349.